

Synthesis and optical properties of starch capped ZnO/ZnS core/shell nanocomposites through chemical bath deposition method

SUJATA DEB*, P. K. KALITA^a, P. DATTA

Department of Electronics Science and Communication Technology, Gauhati University, Guwahati-781014, Assam, India

^aDepartment of Physics, Guwahati College, Guwahati-781021, Assam, India

Starch capped ZnO/ZnS core/shell nanostructures are synthesised by a simple chemical bath deposition (CBD) method at room temperature. In this report, synthesis of ZnO nano tripod structures coated with ZnS shell and their optical properties are presented. Structural characterization is done by X-Ray diffraction (XRD) and high resolution transmission electron microscopy (HRTEM). XRD of the core / shell film shows the presence of diffraction peaks both for ZnO and ZnS. In this work, we have been capable to find the rare hexagonal phase in addition to the cubic phase of ZnS. HRTEM images of ZnO/ZnS nanostructures reveal very vividly the formation of core-shell quantum dots. UV-Vis spectrum exhibits the absorption edge of ZnO/ZnS nanoparticles at about 400nm. With respect to core, core-shell system significantly improved the fluorescence quantum yield but the shell growth is accompanied by a small red shift (5–5.5 nm) of the Excitonic peak in the photo-luminescence (PL) wavelength, suggesting a partial leakage of the exciton into the shell material. Thus, enhanced fluorescence quantum yield due to core/shell nanostructures will bring in possibilities for a wide range of application fields.

(Received February 12, 2013; accepted September 18, 2013)

Keywords: ZnO/ZnS core/shell, Fluorescence Quantum Yield, Red shift, ZnO nano tripod

1. Introduction

Nanostructured materials have been found to show evidence of strange properties, which are entirely dissimilar from their bulk counterparts. Of late, core-shell nanostructures have been found to be the subject of great interests in research due to their interesting properties and potential applications ranging from light-emitting diodes [1] to biological systems [2]. The process of deposition of an additional coat of inorganic material on quantum dots is entitled as shell and such structures quantum dots are widely identified as core / shell quantum dots. In such core/shell structures, the shell has been acknowledged to offer a physical obstacle between the optically active core and the surrounding medium, consequently making the nanostructure not as much of sensitive to environmental variations or surface degradation and other interactions. In addition, the shell provides an effective passivation of the surface trap states, thus increasing heightened fluorescence quantum yield [3]. A lot of core/shell has been reported [4-5]. However, a few results about ZnO based starch capped core-shell nanostructures have been reported up to now. ZnO is a promising II-VI class semiconductor having the energy band gap of about 3.37 eV, corresponding to light emission at wavelength of 368 nm. It has a large exciton binding energy of 60 MeV and is appropriate for short wavelength optoelectronic applications. Besides, ZnO can show a different set of growth morphologies in the nano system that has made this material a promising candidate in the field of nanotechnology [6]. It is reported that

surface modification of a semiconductor with another semiconductor of wide band gap has been accepted as one of the highly developed methods to improve the luminescence properties [7]. ZnS is a wider band gap (3.7eV) material. It has been considered as one of the most important shell materials used for over coating numerous II-VI and III-V semiconductor nanostructures [8-9]. ZnS is an appropriate candidate for ZnO to successfully reduce its band gap and enhance the photocurrent value for the optoelectronic application. Generally, this category of core/shell structure is termed as type I core/shell quantum dots (core with a smaller band gap and shell material with a larger band gap, which confines both electrons and holes in the core). In type II core/shell quantum dots, each carrier type is confined in a different section, meaning that the electrons and holes are spatially separated. However, the core/shell structure of ZnO/ZnS is found to be an exceptional case. Though lower band gap material ZnO is coated with higher band gap material ZnS, but as the band difference between ZnO and ZnS is not sufficiently large, the exciton may not reside in core itself, there may be a leakage to shell region. Hence, this type of structures may be termed as quasi- type II nanocomposite. Thus, because of charge separation, this material has also potential to use in photovoltaic devices. We, here report the synthesis of such quasi-type II core/shell structure by growing a higher band gap ZnS on a lower band gap material ZnO and red shift confirmed the formation of such quasi type II core/shell nanostructures. In the present work, therefore, the amalgamation of ZnO and ZnS in the structure of some

/shell configuration has been demonstrated to progress the optoelectronic properties than either ZnO or ZnS alone. Most of the work in the direction of core-shell has been done by expensive techniques like chemical vapour deposition (CVD), thermal chemical vapor deposition, plasma laser deposition (PLD), hydrothermal deposition and liquid-phase chemical conversion process etc. [10-11]. This work reports a simple chemical bath deposition method (CBD) based room temperature synthesis route using starch as a capping agent which plays a significant role to increase the stable surface passivation or protection [12]. Starch is a natural polymer which possesses many unique properties [13, 14]. Moreover, in this report the synthesis of ZnO nano tripod structures coated with ZnS shell and their optical properties were also presented. ZnO tripod nanostructures were seldom investigated; in fact a number of research works concerning the synthesis and characterization of ZnO nano spherical structures [15] were reported. As it happens, shape oriented nanostructures have larger surface to volume ratios. Spherical nanostructures considered in comparison to be the simplest in shape, however, nanostructures like tripod, tetrapod have larger surface to volume ratios and considered complex. Hence, the surface states of these complex nanostructures are found to govern the optical and electrical properties. It is expected that more absorption may occur which can be used for fabrication of photovoltaic devices. [16] Min-Yeol Choi et al. found to obtain ZnO nano tripods by thermal chemical vapor deposition. Further, the photoluminescence (PL) spectra of ZnO and ZnO/ZnS core/shell structures specify that the PL property can be greatly enhanced by coating ZnO nanostructures with a coating of ZnS, which can be used as an effective layer in LED.

2. Experimental details

2.1 Synthesis

In the present work, two samples of core/shell ZnO/ZnS were prepared by chemical bath deposition method using starch as capping agent. The samples were synthesized for different volume ratio of core to shell material. The ratio of the molar volumes of core ZnO to shell ZnS were 2:1 and 4:1 for sample-1 and sample -2 respectively. The growths of core/shell form of nanostructures were consisted of two steps. The steps were (i) the preparation of core ZnO nanostructures and then (ii) the formation of a ZnS shell coating on it. The chemical reagents used in the synthesis were of analytical grade (Merck) and were used as received without further alteration. Zinc sulphate heptahydrate ($\text{ZnSO}_4 \cdot 7\text{H}_2\text{O}$), thiourea ($\text{NH}_2\text{CS.NH}_2$) and sodium hydroxide (NaOH) were selected to synthesize ZnO/ZnS core/shell nanostructures. In the synthesis, ammonia is used as a complexing agent for preparation at alkaline medium. The whole of the synthesis method (Fig. 1) was carried out in distilled water for being environmentally benign. First, a soluble starch (3%) stock solution was prepared in distilled

water. Then, a 0.5 M solution of Zinc sulphate heptahydrate ($\text{ZnSO}_4 \cdot 7\text{H}_2\text{O}$) was prepared and mixed with the starch solution under constant stirring for good dispersion producing Zn^{2+} ion solution. This solution was divided into two parts. To one part of this starch capped zinc acetate solution, sodium hydroxide (NaOH) solution was mixed drop wise with constant stirring and the resulting solution was heated at 80°C about one and half hour. The colour of the resulting reaction mixture (milky white) confirmed the formation of ZnO. Then, half of this ZnO was kept for core use. Next, a very small amount of ammonia solution was added to the other part of starch capped zinc acetate solution to produce Zn complex solution adjusting pH to 11. This, again was divided into two parts. One part being left for shell use. The other part was mixed with 0.5 M of thiourea to yield ZnS. Next, the ZnO/ZnS core/shell nanostructures were synthesized with respect to change of volume ratio of core and shell matrix solution at 2:1 (sample 1) and 4:1 (sample 2). The synthesis was carried out by taking ZnO matrix solution in a cleaned beaker to which both Zn complex and thiourea were poured alternately drop-wise, the solution which was kept on stirring using a magnetic stirrer at high temperature for about four hrs. (approx.), which resulted in the formation of ZnO/ZnS core/shell nanocomposites. The entire process was performed at ambient atmosphere. Cleaned glass slides were dipped into the resultant matrix solutions to obtain thin films for XRD studies. The samples were also prepared as colloidal solutions for optical as well as HRTEM studies. The samples were stored in airtight desiccators at room temperature for those characteristic studies.

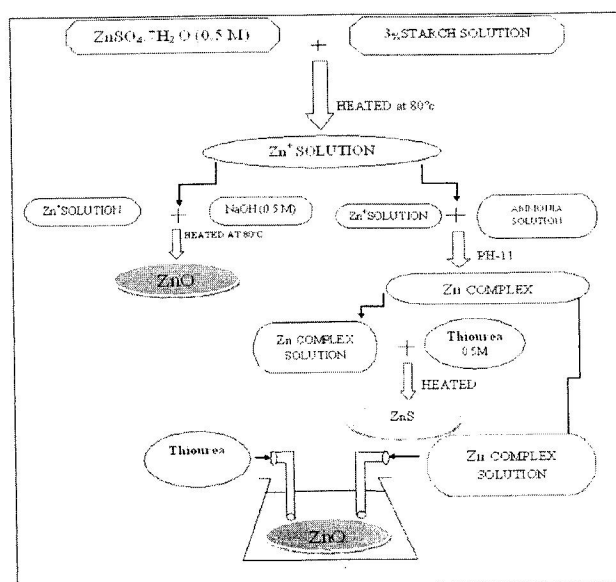


Fig. 1. Block diagram of ZnO, ZnS and ZnO/ZnS (core shell).

2.2 Characterization

The synthesized ZnO and ZnS along with their core/shell structures have been characterized by standard techniques--- X-ray diffractometer (XRD), high resolution transmission electron microscopy (HRTEM), UV-Vis and photoluminescence (PL) spectroscopy. X-ray diffractogram for the synthesized materials was carried out by an XPERT-PRO Philips diffractometer, over an angular range of $15.01^\circ < 2\theta < 80^\circ$ with step scan 0.06 using Cu-K α radiation ($\lambda = 1.54056 \text{ \AA}$). Structural characterizations were recorded on a High Resolution Transmission Electron Microscope (JEOL JEM-2100) operating at 200 KV and the Selected Area Electron Diffraction (SAED) was also developed while HRTEM measurements were done. The Photoluminescence spectra of the samples were recorded using a model-F-2500 FL spectrophotometer, Hitachi with excitation wavelength of 260 nm. The optical absorption spectra were recorded using UV-visible spectrophotometer (a model-UV-1800), Shimadzu in the range 270 nm to 800 nm.

3. Results and discussion

3.1 Structural morphology

The XRD shows the films are polycrystalline and shows the presence of diffraction peaks both for ZnO and ZnS. Fig. 2 shows the XRD pattern of the as-obtained ZnO/ZnS core/shell nanostructures. The lattice parameters are calculated corresponding to respective planes of ZnO which is found to be $a = 3.249 \text{ \AA}$ and $c = 5.207 \text{ \AA}$ which are in good agreement with the standard data. The particle size of ZnO calculated by using well known Scherrer formula is found to be 21.8 nm. The particle sizes indicate the strong quantum confinement of the core ZnO sample. There are dominant peaks at 31.79° , 34.44° and 36.25° which belong to (100), (002) and (101) diffraction planes respectively of wurtzite structured ZnO. The additional planes of ZnO are also formed at $2\theta (= 47.57^\circ, 56.62^\circ, 69.13^\circ, 62.91^\circ$ and $72.65^\circ)$. The observed diffraction planes were in good agreement with the JCPDS file no. 36-1451. Similarly, the shell material ZnS is also confirmed by estimating the respective lattice parameter for respective phases (cubic and hexagonal). It is also observed that ZnS possesses a mixed type of phases having both cubic as well as hexagonal type. From the literature review, it is found that at the interface of core and shell, it is cubic and far away it is hexagonal [17]. The XRD shows the reflections at 28.6° (111), 30° (101), 33.5° (200), 39° (102), 48.5° (220), 59° (004), 59.8° (222), 72.5° (400) and 74.5° (210) for the cubic ZnS blende and the diffraction peaks at 47.737° (110), and 56.622° (118) can be indexed to the hexagonal form of ZnS. This is in agreement with the wurtzite-8H (ICDD reference code: 39-1363) phase, which is supported by earlier reports as well [17]. The diffraction peaks of face centred cubic zinc blende structure with lattice constants $a = 5.406 \text{ \AA}$ are in good agreement with the values in the standard card

(JCPDS file 05-0566). Thus, in this work, we have been capable to find the rare hexagonal phase in addition to the cubic phase. As the peaks of ZnS were more or less at similar position of ZnO, it is found that the peaks were overlapped together in ZnO/ZnS core-shell nanostructures. A broad peak at around 42° may perhaps be correlated to a distorted structure of ZnS that can be related to reflections from the (1 010) planes and the other peak at 51.231° may be due to reflections from the (1 0 12) planes. This can be related to enhancement of surface states as discussed in the optical analysis. Other earlier workers have also discussed the same enhancement of surface states [17]. They also found the effect of surface states because of distortion of planes.

To study the structural information in details, HRTEM was done. The high-resolution TEM (HRTEM) image of as-prepared ZnO/ZnS structure shows the strong contrast between the core and the -shell nanostructure [Fig. 3 and Fig. 4]. The structural morphology clearly shows that the tripod type ZnO core nanoparticles are coated with the spherical ZnS shell nanoparticles. The tripod type ZnO is also reported by other workers preparing by thermal chemical vapour deposition method [18]. Because of anisotropic growth preferably in the (001) direction this type of tripod ZnO nanoparticle is found. The particle distribution reveals that the core/shell nanocomposites have a tendency to agglomerate to form bigger structures. The SAED (Fig. 3d) patterns of composites exhibit the presence of ZnO core and ZnS shell diffraction planes. The images clearly show the d-parameter 0.52 nm is corresponding to (001) planes of ZnO and that of 0.31 nm corresponding to (111) ZnS, shell. ZnO can react with sulphide ions released from $\text{NH}_2\text{CS.NH}_2$ and convert into ZnS over ZnO core. Figure 3a shows the structures with almost uniform shell coating. The SAED of an individual ZnO/ZnS core/shell structures displays a set of diffraction rings belong to polycrystalline ZnO core and ZnS nanoparticles. Similar type SAED patterns of ZnO/ZnS core /shell nanostructures have been reported by different workers [19].

3.2 Optical properties

The UV-vis. absorption spectrum of ZnO/ZnS core-shell nanostructure has been depicted in Fig. 5. It shows quite noise type absorption around 400nm. This may be due to the additional oxide formation because of atmospheric oxidation. Atmospheric oxidation generally occurred in open air chemical synthesis process, as revealed by other workers as well [17]. As a result the composites become ZnO/ZnS/ZnO which influences the absorption edge owing to those surface states. The absorption peaks clearly red shifted corresponding to absorption for ZnO core. The additional distinct absorption appeared at 550 nm & 565 nm are expected due to impurities preferably the oxygen interstitials. This is also supported by the additional green emission of the PL spectra of ZnO as well as ZnO/ZnS (Fig. 6). With respect to core, core-shell system exhibited enhanced photoluminescence (Fig. 6). Here, the shell growth

reduced the number of surface unsaturated bonds or dangling bonds, which can act as trap states for charge carriers and thereby reduce the fluorescence quantum yield. The ZnS shell thus significantly improved the fluorescence quantum yield. The PL emission peaks of ZnO and ZnS are found to be at 396.5 nm and 339.5 nm. Photoluminescence investigation evidenced the strong emission bands at about 400.5 nm (ZnO: ZnS=2: 1, sample-1) and 401.0 nm (ZnO: ZnS=4: 1, sample-2). It shows that shell growth is accompanied by a clear red shift (5–5.5 nm) of the excitonic peak in the photoluminescence (PL) wavelength corresponding to bare core ZnO; however the red shift is very small which is in consistent with the type I core-shell nanostructures. This observation can be attributed to a partial leakage of the exciton into the shell material. The red shift of core/shell nanostructure over the core is in well agreement with those reported by other workers [15, 20]. S. Chattopadhyay et al. also inferred that in small core/shell quantum dots, tunnelling and spreading of the carrier particles over the shell region is more probable and can be the main reason behind the red-shift in PL spectra. Thus, we observed that smaller the core / shell nanostructures, greater the PL intensity with a red-shift in PL spectra. Earlier report of the study of CdS/ZnS wires also evidenced the enhanced PL emission of core/shell structures [21, 22]. Moreover, in this work, the PL intensity of as-prepared core/shell of composition ZnO: ZnS=2: 1 has also enhanced over the composition ZnO: ZnS=4: 1 (Fig. 6). Thus, ZnO/ZnS core/shell is behaving more like quasi- type -II core/shell nanostructures with enhanced PL, accompanied by a small red - shift. In addition, the strong band gap emission demonstrates the high crystalline nature of the as-synthesized particles. Usually two emission peaks are observed in semiconductor nanocrystals - the exciton and the trapped luminescence. It is seen that the exciton emission peak is sharp and the trapped emission is wide. The source of the violet and green emission may possibly be attributed to the defect-related emissions between Zn interstitial and vacancies; O interstitial and vacancies respectively. The PL spectra of ZnO/ZnS core-shell structures are evidence for a superior broad violet emission and weakened green emission compared to that of ZnO nanostructures. The enhancement in violet emission can be attributed to the fact that ZnS nanoparticles has a higher band gap compared to ZnO nanoparticles and the tunnelling of the charge carriers from the core to the ZnS nano shell was almost concealed and henceforth, more number of photo generated electrons and holes are found to get confined inside the ZnO core, resulting to an elevated quantum yield compared to individual nano ZnO. However, it is observed that the green emission is weakened to a huge degree. As it is known that the green emissions initiate from oxygen interstitials and vacancies. During the course of action of the configuration of ZnO/ZnS core-nanostructures, the sulphur atom can swap and squeeze out the oxygen interstitials from the surface of ZnO nanoparticles. Consequently, the concentration of oxygen interstitial is reduced significantly and the green emission is weakened. Thus it is indicated that the

sulfidation process has an immense effect on the relative intensity and location of characteristic PL properties of ZnO nano crystals. Many earlier workers have also concluded the same [23]. We find on the surface of ZnO a lot of surface unsaturated bonds that form the gap surface states. So, the fraction of the electrons that are excited to the conduction band would first move to the surface states that are in the middle band gap, and then will recombine nonradiatively with the holes lying in the valence band, likewise dropping the emission intensity. Hence the surface traps of ZnO can be passivated if a shell of higher-band-gap material ZnS be capped, such that the chance of the nonradiative recombination of the surface states would reduce , contributing appreciably to increased PL intensity. Thus, the PL properties of ZnO nanoparticles possibly will be adjusted by this scheme.

From the above observations, we can conclude that the intensity of UV emission was obviously enhanced after a thin layer of ZnS was coated on bare ZnO. Therefore, these ZnO/ZnS core/shell nanostructures are more applicable for the fabrication of optoelectronic devices, such as UV light-emitting diodes.

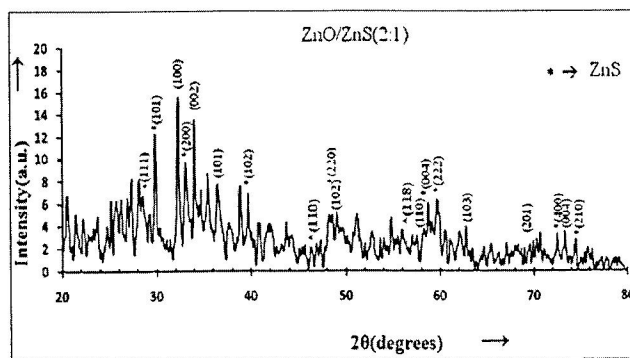


Fig. 2. XRD pattern of ZnO/ZnS(2:1) nanoparticles.

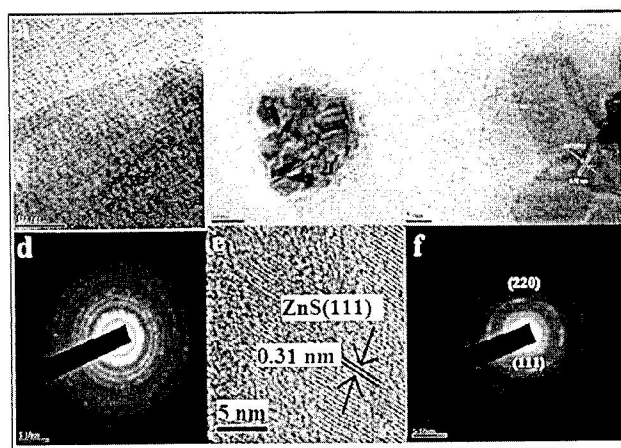


Fig. 3. (a), (b) and (c) showing HRTEM Images of ZnO/ZnS core/shell and (d) showing corresponding SAED pattern and (e) HRTEM image of ZnS shell and (f) its SAED pattern.

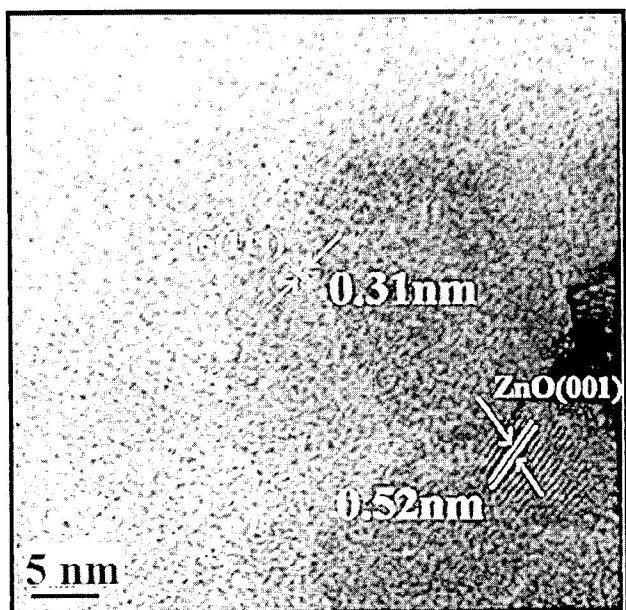


Fig. 4. Showing magnified picture of Fig. 3 (c) HRTEM images of ZnO/ZnS core/shell.

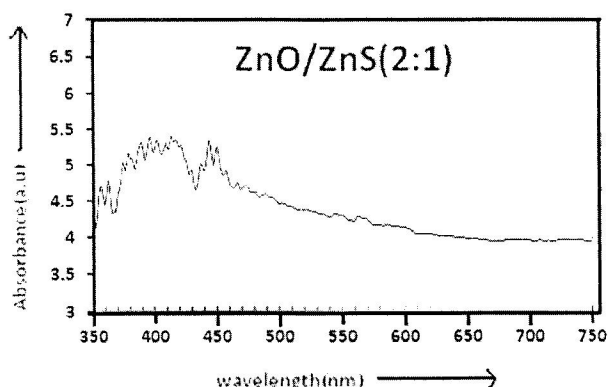


Fig. 5. UV spectra of ZnO/ZnS nanoparticles.

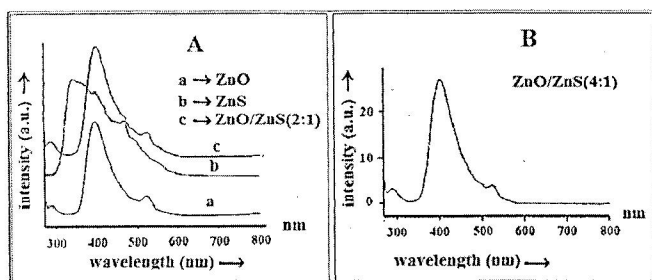


Fig. 6. (A) PL emission spectra of ZnO, ZnS, ZnO/ZnS(2:1) and (B) PL emission spectra of ZnO/ZnS(4:1) nanoparticles.

4. Conclusion

In summary, ZnO, ZnS and ZnO/ZnS were simultaneously synthesized under the same growth conditions by a simple chemical bath deposition method.

The method is in general a cost-effective one which has the potential to produce functional core/shell type semiconductor nanocomposites with a number of compositions and shapes for unique properties. In the present synthesis, starch was found to be a good capping material for producing core-shell composite. The synthesized ZnO and ZnS along with their core/shell structures have been characterized by XRD, HRTEM, UV-Vis and PL spectroscopy. The XRD shows the presence of both hexagonal ZnO and mixed type ZnS in core / shell nanostructure. In this work, we have been capable to find the rare hexagonal phase in addition to the cubic phase of ZnS. The HRTEM morphology shows the formation of ZnO/ZnS nanostructure having a tripod type core. UV-Vis spectrum exhibits the absorption edge of ZnO/ZnS nanoparticles at about 400nm which is in consistent with emission spectra. It is also reported in the present work that the PL spectra of ZnO and ZnO/ZnS core/shell structures specify that the PL property can be greatly enhanced by coating ZnO nanostructures with a coating of ZnS shell. The PL spectra of ZnO and core-shell clearly exhibit the near band gap emission around 396.5 nm, 400.5 nm (for composition ZnO: ZnS=2: 1) and 401.0 nm (for composition ZnO: ZnS=4: 1) respectively. This also shows a clear small red-shift that is attributed to the formation of core/shell. An additional green emission around 550 nm owing to impurities preferably the oxygen interstitials. The PL intensity of as- prepared core /shell for composition ZnO: ZnS=2: 1 was also found to be enhanced in comparison to that of composition ZnO: ZnS=4: 1. The ZnO/ZnS core/shell nano rods exhibit a distinct UV enhancement in luminescence as compared to that of the uncoated ZnO nanowires as a result of the passivated nonradiative recombination sites. Therefore, this strategy might open up an opportunity for extensive study of the physical and chemical properties of other semiconductor core/shell and hollow structures with various compositions and morphologies, broadening their potential applications in electronics, magnetism, optics, catalysis, mechanics, electrochemistry, sensors, etc. Therefore, the chemical growth of ZnO, ZnS and ZnO/ZnS nanostructures prepared with their volumetric ratios may results newer novel photoluminescence properties that can be used in fabrication of light emitting devices.

Acknowledgements

The authors gratefully acknowledge the technical support of G.U., IIT, Guwahati and SAIF, Shillong.

References

- [1] H. Kim et al., *J. Cryst. Growth*, **326**, 90 (2011).
- [2] M. Tomadakis, K. Mitra, Proc. 3-rd Inter. AIP Conf. Porous media and its applications in science, engineering and industry, Montecatini, Italy, 2010, p.181.
- [3] A. Emamdoust, S. F. Shayesteh, M. Marandi,

- Pramana- J. Phys., **801**, 713 (2013).
- [4] F. Ruffino, A. Pugliara, E. Carria, C. Bongiorno, M. G. Grimaldi, Phys. E, **47**, 25 (2013).
- [5] A. M. Suhail, A.N. Naje, R. R. Mohammed, G. S. Muhammed, Proc. 7-th Inter. INCOSOL Conf. on Solar energy for MENA region, Amman, Jordan, 23 (2012).
- [6] J. Grabowska et al., Phys. Rev. B, **71**, 115439 (2005).
- [7] J. Li et al., J. Phys. Chem. B, **110**, 14685 (2006).
- [8] P. Verma, A. C. Pandey, J. Biomater Nanobiotechnol, **2**, 409 (2011).
- [9] H. Yang, H. P. Holloway, Appl. Phys. Lett., **82**, 4633 (2003).
- [10] X. Huang et al., ACS Nano, **6**, 9347 (2012).
- [11] L. Liu et al., ACS Appl. Mater. Interfaces, **4**, 17 (2012).
- [12] P. R. Gopalan, A. G. Annaselvi, P. Subramaniam, Dr. P. R. Gopalan, Int. J. Nanomater. Bios., **3**, 26 (2013).
- [13] M. Vert, I. D. Santos, S. Ponsart, N. Alauzet, J-L. Morgat, J. Coudance, H. Garreau, Polym. Int., **51**, 840 (2002).
- [14] D. R. Lu, C. M. Xiao, S. J. Xu, Express Polym. Lett., **3**, 366 (2009).
- [15] Y. F. Zhu, D. H. Fan, W. Z. Shen, J. Phys. Chem. C, **112**, 10402 (2008).
- [16] M-Y. Choi, H-K. Park, M-JinJin, D. H. Yoon, S-W. Kim, J. Cryst. Growth, **311**, 504 (2009).
- [17] N. Goswami, P. Sen, J. Nanopart. Res., **9**, 513 (2007).
- [18] S. Mandal, A. Dhar, S. K. Ray, J. Appl. Phys., **105**, 033513 (2009).
- [19] R. Yi, G. Qiu, X. Liu, J. Solid State Chem. **182**, 2791 (2009).
- [20] S. Chattopadhyay, P. Sen, J. T. Andrews, P. K. Sen, J. Phys.: Conf. Ser., **365**, 012037 (2012).
- [21] A. Datta, S. K. Panda, S. Chaudhuri, J. Phys. Chem. C, **111**, 17260 (2007).
- [22] R. G. Xie, U. Kolb, J. X. Li, T. Basche, A. Mews, J. Am. Chem. Soc., **127**, 7480 (2005).
- [23] G. Rani, P. D. Sahare, Nano Commun. Netw., **3**, 197 (2012).

*Corresponding author: sujatabmk@gmail.com